National Research Institute of Papua New Guinea – 6-Month Cruise Report for WV0103 (January 2003 cruise aboard the R/V *Western Venturer*)

Marine Sedimentation of the Fly River, Papua New Guinea

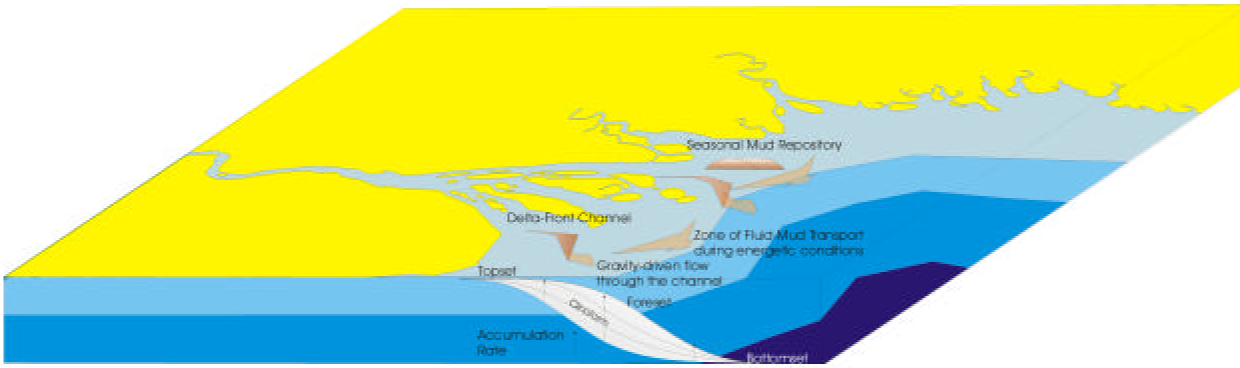

Charles A. Nittrouer[1], Andrea S. Ogston[1], Miguel A. Goni[2]

1. University of Washington, School of Oceanography, Box 357940, Seattle, Washington, USA
2. University of South Carolina, Department of Geological Sciences, 701 Sumter Street, Columbia, South Carolina, USA

Introduction

Clinoforms – sigmoidal-shaped deposits on the continental shelf – have been recognized as the basic building blocks of continental margin morphology (Mitchum, 1977). Clinoforms are observed on many margins both ancient (e.g., Asquith, 1970; Leithold, 1993) and modern (e.g., Nittrouer, et al., 1986a; Kuehl et al., 1989; Alexander et al., 1991) and high-rates of sediment supply make them common in wet tropical environments (e.g., Nittrouer et al., 1996). Even though clinoforms are common features throughout the world, the sedimentary processes that lead to the formation of these deposits are still unclear. By studying the contemporary evolution of the clinoform deposit in the Gulf of Papua, Papua New Guinea, this research will maximize the global significance of the results, and enhance our understanding of the geologic record (e.g., Mount, 1984; Cowan and James, 1993; Whalen et al., 2000).

The study site was chosen because of the global significance of tropical rivers. Rivers located in wet-tropical environments (e.g., Indo-Pacific, west-central Africa, northeast South America) are recognized as important contributors to the global budgets of freshwater ($19 \times 10^3 km^3$, 51% of the world total), particulates (16×10^9 metric tons – more than 60% of the world total), and dissolved organic carbon (65% of the world total) (Meybeck, 1988). Insights gained from the study of the wet tropics have far-reaching implications because of the volume of oceanic material derived from these environments.

The ultimate fate of sediment depends strongly on the processes that cause sediment to accumulate. Sediment discharged on tropical margins can act as carriers for other chemical constituents such as organic carbon and pollutants. The reactive surfaces of sediment particles provide sorption sites for contaminants (Ongley et al., 1992) and particle motion accounts for the transport of over 90% of sedimentary organic carbon (Hedges and Keil, 1995). The processes that transport sediment can have a direct impact on the chemistry and cycling of carbon and other sedimentary constituents (Aller and Blair, 1996), and understanding the dispersal of sediment on continental margins provides insight to the distribution of organic carbon and particle-reactive contaminants in the marine environment.

Synergistic effects of winds, waves, tidal currents, and sediment supply conspire to create clinoforms. Energetic oceanic conditions on the shallow topset inhibit sedimentation, and sediment is transferred to the relatively steep, but deeper foreset where accumulation rates are highest. Because most sediment accumulates on the foreset, low sediment supply on the bottomset results in relatively slow accumulation and flat morphology (on the pre-existing transgressive surface). Correlation between the rollover (i.e., topset – foreset boundary) of the clinoform and a reduction in wave and tide-induced shear stress has been noted (Walsh et al., in press), but no mechanism for mobilizing sediment and transporting it to the foreset has been identified. Fluid mud (i.e., suspended-sediment concentrations >10 g/l) has been suggested as a vehicle for transferring sediment from the topset to the foreset of the Fly clinoform (Harris et al., 1993) but it has not been studied yet.

Fluid-mud transport has received increased attention due to its unexpected presence on margins throughout the world (e.g., Amazon River – Kineke et al., 1996; Kuehl et al., 1996; Eel River – Ogston et al., 2000; Traykovski et al., 2000), and fluid-mud accumulation is a focus of this study. The objective of the January 2003 cruise aboard the R/V Western Venturer was to collect samples from shallow areas that cannot be accessed by larger research vessels. In order to gain insight into the processes that lead to the formation of the clinoform, the sedimentary characteristics (e.g., structural, radiochemical, grain-size) of the deposits near the Fly River were described within the context of gravity-driven transport. In addition, physical oceanographic parameters (e.g., salinity, temperature, currents) and chemical parameters of the sediments (e.g., % organic carbon, % total nitrogen, del$^{13}C_{oc}$) were measured in order to facilitate a broad understanding of the Gulf of Papua clinoform system.

The RV *Western Venturer* sailed from Port Moresby on January 6, 2003 and returned to Port Moresby on January 19, 2003. These dates encompassed a period during the typically quiescent monsoon season in the Gulf of Papua. In addition, 2003 is a year affected by moderate El Nino conditions causing low flow in the Fly River. The cruise embarked with scientists Chuck Nittrouer, Andrea Ogston, Wayne McCool, John Crockett, and Deborah Nittrouer from the University of Washington, Miguel Goni, and David Shelley from the University of South Carolina, Joel Rowland from the University of California, Berkeley, and Marie Bera from the University of Papua New Guinea. In this preliminary report, current results are presented with a brief discussion of how those results are shaping future research plans.

Methods

Seabed sampling was accomplished by using a 3-m long coring device (kasten corer), a Shipek grab sampler, and the Boundary Layer in Situ Sediment Profiler (BLISSP) that measured salinity, temperature, and water depth, and collected samples of suspended sediment using underwater pumps. Sediment samples were photographed to reveal internal sedimentary structures. In addition, the activity of natural radioisotopes (^{210}Pb) and grain size were measured at University of Washington laboratories. ^{210}Pb activities are commonly used to estimate accumulation rates of sediment.

A benthic tripod was deployed at location CT (Fig. 1) for eight days in the Far North Entrance of the Fly River. This instrument measured salinity, temperature, and currents continuously for its entire deployment. It also measured pressure at the seabed from which wave height was calculated.

Bathymetry was measured along the delta front of the Fly River using a Garmin fathometer linked to a GPS. This experiment was designed to locate and describe across-shelf channels located on the delta front that could act as conduits, transporting sediment into deeper water. Several uncharted channels were identified (Fig. 2) and sampled with both coring devices and the BLISSP. Cores and samples were analyzed for sedimentary structures and ^{210}Pb activities were measured.

The BLISSP and ADCP (Acoustic Doppler Current Profiler) were used in conjunction in the Far North Channel at 'Anchor' station (Fig. 1) to resolve the sediment supply dynamics of the Fly River over a tidal cycle. The station was occupied at anchor for 7.5 hours during which time the ADCP collected water-column velocity data continuously and the BLISSP was deployed every 0.5h to measure suspended sediment in the water column, as well as the other water properties.

For all sediment samples, both from the seabed and the water column, Miguel Goni collected samples to measure total and organic carbon content, nitrogen content, and the distribution of the stable isotopes of both elements.

Results

A total of 77 stations were occupied (Fig. 1, Table 1) covering areas to the north of the river mouth, directly in front of the river mouth, and in the Fly River delta. Core FF3 is representative of the cores collected north of the river. The core is dominated by physical structure with no evidence of bioturbation (Fig. 3). ^{210}Pb activities vary considerably in the surface mixed layer that extends down to ~30 cm (Fig. 4). Below that, logarithmic decay of activities indicates an accumulation rate of 1.5 cm/y. Core CT taken from the axis of a channel that incises the Far North Entrance (Fig. 1) shows a different profile. Although it is also dominated by physical structures (Fig. 5), the ^{210}Pb profile shows a sharp decrease in activity at ~150 cm depth (Fig. 6).

The tripod, also deployed at station CT, shows currents oriented approximately northwest-southeast, or along the channel (Fig. 7). Increased suspended sediment measured by the Optical Backscatterometer (OBS) correlates with increased wave and tide energy during spring tide. Water column properties at the Anchor station (Fig. 8) demonstrate the migration of a turbidity maximum over the course of one tidal cycle.

Sediments from both north of the river mouth and in front of the delta were characterized by relatively low organic carbon content (%OC), with the lowest values measured in the central part of the delta front study area (0.4 to 0.8 %OC) (Fig. 9). Notably, higher %OC values were measured in sediments off the tip of Kiwai Island. The highest %OC contents were measured in the eastern and western ends of the delta front region (1.0 to 1.2 %OC and 1.0 to 1.8 %OC, respectively), with the maximal values off Parana Island. In contrast, the northeast region showed less variable compositions with most stations displaying values of 1.0 to 1.4 %OC. The only exceptions were the sediment from one of the stations along the transect off Bell Point, which gave low values (0.4 %OC), and the sediment from the station immediately to the northeast, which was high in OC (1.8 %OC).

The atomic carbon:nitrogen ratios ([C:N]a) of sediments from both regions (Fig. 10) also displayed significant spatial variability, although all the measured values were overall elevated (12 > [C:N]a > 24). In the delta front, sediments from the region between Kiwai and Cmuda Islands were characterized by relatively low [C:N]a ratios (12 to 14), whereas the sediments from the western region of the delta front area displayed significantly higher ratios (16 > [C:N]a > 24). Some of the sediments off the south channel of the Fly River (between Kiwai and Mibu Islands) were an exception, yielding low [C:N]a ratios (~14). The highest [C:N]a ratios of this region of the delta front were measured off Parana Island, with values ranging up to 24. The sediments from the northeast region, in contrast to the trends in %OC (Fig. 9), displayed significant spatial variability. The western portion of this study area, located off the North Channel of the Fly River and off the mouths of the Bamu and Turama Rivers, contained sediments characterized by low [C:N]a ratios (12 to 14), while sediments from the eastern offshore portions of the study area displayed higher ratios (16 to 24).

The del$^{13}C_{OC}$ compositions of surface sediments from both study areas displayed relatively depleted values that ranged from -24‰ to -27‰ (Fig.11). In the delta front area, sediments from the central region yielded the most enriched signatures (-24‰ to -24.5‰) of the whole Fly River Delta. The location of these sediments coincides with those that yielded the low %OC and [C:N]a values. Most of the rest of the sediments in the delta front region yielded ?$^{13}C_{OC}$ compositions that ranged between from -25‰ and -25.5‰. In contrast, virtually all the sediments in the northeast region yielded more depleted del$^{13}C_{OC}$ values (-26‰ to -27‰). The major exception was sediments from the station off Bell Point, which contained sediments with low %OC (Fig. 9), which were characterized by a significantly enriched del$^{13}C_{OC}$ value of -24.5‰.

Discussion

The delta front of the Fly River exhibits morphological diversity that appears to influence the sedimentary regimes present there. In addition, seasonal variations in winds and waves contribute to the processes that control sediment transport. The preliminary results presented here are relevant for the quiescent monsoon season during which they were collected, but may not extend to all energy regimes present in the GOP.

The area north of the river mouth is presently accumulating sediment on the 100-year time scale measured by ^{210}Pb. This is most likely a result of sediment transport directly out of the Fly River that is subsequently influenced by the general northeastward circulation hypothesized to be present as a result of the Coral Sea Current. Sediment discharged by the river can be transported north of the river mouth where some of it accumulates and some is temporarily deposited. The relatively deep surface mixed layer (~30 cm, Fig. 4) indicates that waves and tidal currents frequently resuspend sediment. The instability of the seabed due to the physical stresses inhibits colonization by benthos and leads to the preservation of the physical structures observed (Figs. 3,5). The zone of accumulation corresponds to a decrease in porosity (data not shown) implying that the SML is kept relatively unconsolidated and available for transport by resuspension events. We hypothesize that this process is vital to maintaining a large pool of sediment available for transport as highly concentrated (> 10g/l) fluid muds during the more energetic trade-wind conditions.

Within the channels that incise the delta front (Fig. 2), it appears that a different process may operate. Core CT also displays physical stratification that is unaltered by biological processes (Fig. 5) showing that the physical stresses preclude any benthic communities. However, the abrupt decrease in ^{210}Pb activity indicates a horizon of erosion or non-deposition. Our interpretation is that sedimentation within the channels is highly episodic and driven primarily during energetic trade-wind periods. High sediment concentrations converging within the channels that coincide with large waves and tidal currents can produce gravity-driven flows that are competent to erode the underlying seabed and transport sediment beyond the confines of the channel. An alternate regime produces high sediment concentrations that flow out of the estuarine turbidity maximum and are deposited within the channel. The coexistence of these two sediment transport processes can create the observed ^{210}Pb profile. The background sediment has been deposited beyond the time scale measured by ^{210}Pb (>100 y) and exhibits only background activity. That layer has been eroded by energetic gravity-driven flows creating the sharp contact. Above the contact (in the case of core CT at ~150 cm) a plug of sediment has been deposited in a relatively short amount of time, and therefore has a constant activity that is higher than the background value. Finally, the surface sediment (the top 20 cm) has been reworked by currents and waves in the channel, and has a variable activity as a result of the reworking.

Currents within the channel are dominantly tidal in nature and oriented along the axis of the channel. The correlation of suspended sediment with strong ebb tides during spring tide indicates that the currents act to transport sediment down-channel during spring tides. In addition, the observed estuarine turbidity maximum can contribute to suspended-sediment concentrations that enhance gravity-driven flows.

The surface sediments collected in the regions directly offshore from the north and south entrances are characterized by relatively low %OC contents typical of most clastic-dominated environments (e.g. Ruttenberg and Goni, 1997; Gordon et al., 2001). In spite of the overall low %OC values, there are contrasts in the abundance of organic matter between the two study regions. The higher sedimentary OC contents in northeast region may be due to the finer texture of the sediments deposited there relative to those in the central area of the delta front region (Keil et al., 1994). Additionally, the northeast region may have accumulated freshly deposited materials from the river, which have yet to be winnowed and transported elsewhere.

The high [C:N]a and depleted del$^{13}C_{OC}$ values of sediments from both regions indicate that a large fraction of the organic matter originated from terrigenous C_3 plant sources (Fig. 12). Terrigenous C_3 vascular plants are characterized by high [C:N]a and depleted del$^{13}C_{OC}$ values (e.g. Hedges et al., 1986; Goni et al., 1998). A few of the samples display compositions that are consistent with high contributions from relatively fresh C3 vascular plant sources. These are the sediments from the stations offshore from Parama Island in the delta front region and the sediments from the deeper part of the eastern part of the northeast region, off shore from the mouth of the Turama River (Fig. 10). In contrast, most samples plot within the area characteristic of soils with C_3 vegetation (e.g. Hedges et al., 1986). Hence, this result indicates that the majority of the organic matter deposited offshore the Fly River Delta probably originated from tropical rainforest soils (C_3 plants are the dominant vegetation of humid tropical forests; Kastner and Goni, 2003) in the Fly River drainage basin. A few of the sediments display relatively low [C:N]a and enriched del$^{13}C_{OC}$ values, which suggest a small contribution from marine algal sources. These samples are from the northern most offshore area of the delta front region and from the area just offshore from the Turama River in the northeast region.

Overall, the organic geochemical analyses point to the deposition of predominantly clastic-rich particles with relatively low amounts of the OC as the major process responsible for the compositions of Fly River Delta sediments. Furthermore, the tropical C_3 forest vegetation signal of the organic matter in the soils indicates that the origin of these particles is likely to be soils from humid regions of the drainage basin. The predominance of the Fly River as a source of sediments and organic matter to this area is consistent with the very low algal carbon abundances that are evident from the geochemical data. Future studies on the molecular level compositions of these sediments will help us better address the specific sources and diagenetic state of the organic matter in this region of the Gulf of Papua.

Conclusions

During monsoon conditions, sediment discharged by the Fly River has a number of transport pathways. Some is transported to the northeast and is deposited there. Tidal currents and waves contribute to physical mixing and resuspension of the sediment maintaining a substrate too unstable for biological communities. The physical processes inhibit consolidation of the sediment, making it available for offshore transport by fluid muds during more energetic conditions. Sediment is also transported through channels that incise the delta front. Occasionally, gravity-driven flows can erode the seabed creating a stepped ^{210}Pb profile. Large amounts of sediment can be deposited in a relatively short amount of time within the channels, possibly enhanced by processes associated with the estuarine turbidity maximum. Surface sediments within the channels continue to be reworked by waves and currents down to ~20 cm, and currents act to transport sediment down-channel during spring tides.

Chemical signatures of the sediment suggest that the northeast area may be receiving relatively fresh material from the river that is not winnowed or transported farther during the quiescent monsoon. [C:N]a and del$^{13}C_{OC}$ values suggest that much the predominant sediment is clastic rich with relatively low amount of OC. Most of the organic material supplied by the river comes from tropical rainforest soils within the Fly River drainage basin, with a minor contribution from marine algal sources.

Acknowledgements

The RV *Western Venturer* and her crew provided a unique opportunity to sample in and around the Fly River. We acknowledge the generous logistical help provided by Jim Veness and Ok Tedi Mining Limited. We also would like to recognize Marie Bera, Hugh Davies, and Sioni Sioni of the University of Papua New Guinea who were extremely helpful in making this cruise a success.

John S. Crockett and Wayne W. McCool performed preparation and analyses of sedimentary samples and oceanographic data supported through NSF grant OCE-2-3351.

The preparation and analyses of the chemical samples were carried out by Natalie Monacci, Becca Clinton and Rachel Gishewhite. Details on the analytical techniques are available in published papers by Goni and co-workers (1998; 2000). Funding for this work was through NSF grant OCE-0220600.

References

Alexander, C. R., DeMaster, D.J., Nittrouer, C.A., 1991. Sediment accumulation in a modern epicontinental-shelf setting: the Yellow Sea. *Marine Geology* 98: 51-72.

Aller, R. C., Blair, N.E., 1996. Sulfur diagenesis and burial on the Amazon shelf: Major control by physical sedimentation processes. *Geo-Marine Letters* 16: 3-10.

Asquith, D. O., 1970. Depositional topography and major marine environments, Late Cretaceous, Wyoming. *American Association of Petroleum Geologists Bulletin* 54: 1184-1224.

Cowan, C.A., James, J.P., 1993. The interactions of sea-level change, terrigenous-sediment influx, and carbonate productivity as controls on Upper Cambrian Grand Cycles of western Newfoundland, Canada, Geological Society of America Bulletin 105, 1576-1590.

Goñi M. A., Ruttenberg K. C., and Eglinton T. I. (1998) A reassessment of the sources and importance of land-derived organic matter in surface sediments from the Gulf of Mexico. *Geochimica et Cosmochimica Acta* 62, 3055-3075.

Goñi M. A., Yunker M. B., Macdonald R. W., and Eglinton T. I. (2000) Distribution and sources of organic biomarkers in Arctic sediments from the Mackenzie River and Beaufort shelf. *Marine Chemistry* 71, 23-51.

Gordon E. S., Goñi M. A., Roberts, Q. N., Kineke, G. C., and Allison, M. A. (2001). Organic matter distribution and accumulation on the inner Louisiana Shelf. *Continental Shelf Research*. *Continental Shelf Research* 21, 1691–1721.

Harris, P. T., Baker, E.K., Cole, A.R., Short, S.A., 1993. A preliminary study of sedimentation in the tidally dominated Fly River Delta, Gulf of Papua. *Continental Shelf Research* 13: 441-472.

Hedges, J.I., Clark, W.A., Quay, P.D., Richey, J.E., Devol, A.H., de M. Santos, U., 1986, Compositions and fluxes of particulate organic material in the Amazon River: Limnology and Oceanography, v. 31, p. 717-738.

Hedges, J. I., Keil, R.G., 1995. Sedimentary organic matter preservation: an assessment and speculative synthesis. *Marine Chemistry* 49: 81-115.

Kastner T. P. and Goñi M. A. (2003) Constancy in the vegetation of the Amazon Basin during the Late Pleistocene: Evidence from the organic matter composition of Amazon Deep Sea Fan sediments. *Geology* 31, 291-294.

Keil, R.G., Tsamakis, E., Fuh, C.B., Giddings, J.C. and Hedges, J.I., 1994. Mineralogical and textural controls on the organic composition of coastal marine sediments: Hydrodynamic separation using SPLITT-fractionation. Geochimica et Cosmochimica Acta, 58: 879-893.

Kineke, G. C., Sternberg, R.W., Trowbridge, J.H., Geyer, W.R., 1996. Fluid-mud processes on the Amazon continental shelf. *Continental Shelf Research* 16: 667-696.

Kuehl, S. A., Hariu, T.M., Moore, W.S., 1989. Shelf sedimentation off the Ganges-Brahmaputra river system: evidence for sediment bypassing to the Bengal fan. *Geology* 17: 1132-1135.

Kuehl, S. A., Nittrouer, C.A., Allison, M.A., Faria, L.E.C., Dukat, D.A., Jaeger, J.M., Pacioni, T.D., Figueiredo, A.G., Underkoffler, E.C., 1996. Sediment deposition, accumulation, and seabed dynamics in an energetic fine-grained coastal environment. *Continental Shelf Research* 16: 787-815.

Leithold, E. L., 1993. Preservation of laminated shale in ancient clinoforms: comparison to modern subaqueous deltas. *Geology* 21: 359-362.

Meybeck, M., 1988. How to establish and use world budgets of riverine materials. In: Lerman, A., Meybeck, M. (Eds.), Physical and Chemical Weathering in Geochemical Cycle, The Hague, Kluwer Academic: 247-272.

Mitchum, R. M., Jr., Vail, P.R., Sangree, J.B., 1977. Seismic stratigraphy and global changes of sea level, part 6: stratigraphic interpretation of seismic reflection patterns in depositoinal sequences. In: C. E. Payton (Ed.), Seismic stratigraphy - applications to hydrocarbon exploration. Tulsa, American Association of Petroleum Geologists: 117-133.

Mount, J. F., 1984. Mixing of siliciclastic and carbonate sediments in shallow shelf environments. Geology 12: 432-435.

Nittrouer, C. A., DeMaster, D.J., Kuehl, S.A., Kowsmann, R.O., 1986a. The deltaic nature of Amazon shelf sedimentation. *Geological Society of America Bulletin* 97: 444-458.

Nittrouer, C. A., Kuehl, S.A., Figueiredo, A.G., Allison, M.A., Sommerfield, C.K., Rine, J.M., Faria, E.C., Silveira, O.M., 1996. The geological record preserved by Amazon shelf sedimentation. *Continental Shelf Research* 16: 817-841.

Ogston, A. S., Cacchione, D.A., Sternberg, R.S., Kineke, G.C., 2000. Observations of storm and river flood-driven sediment transport on the northern California continental shelf. *Continental Shelf Research* 20: 2141-2162.

Ongley, E. D., Krishnappan, B.G., Droppo, I.G., Rao, S.S., Maguire, R.J., 1992. Cohesive sediment transport: emerging issues for toxic chemical management. *Hydrobiologia* 235: 177-187.

Ruttenberg K. C. and Goñi M. A. (1997) Phosphorous distributions, C:N:P ratios, and del^{13}Coc in arctic, temperate, and tropical coastal sediments: tools for characterizing bulk sedimentary organic matter. *Marine Geology* 139, 123-145.

Traykovski, P., Geyer, W.R., Irish, J.D., Lynch, J.F., 2000. The role of wave-induced density-driven fluid mud flows for cross-shelf transport on the Eel River continental shelf. *Continental Shelf Research* 20: 2113-2140.

Walsh, J.P., C.A. Nittrouer, C. Palinkas, A.S. Ogston, R.W. Sternberg, and G.J. Brunskill. In Press. Clinoform mechanics in the Gulf of Papua, New Guinea. *Continental Shelf Research.*

Whalen, M.T., Eberli, G.P., Van Buchem, F.S.P., Mountjoy, E.W., Homewood, P.W., 2000. Bypass margins, basin-restricted wedges, and platform-to-basin correlation, Upper Devonian, Canadian Rocky Mountains: implications for sequence stratigraphy of carbonate platform systems. *Journal of Sedimentary Research* 70, 913-936.

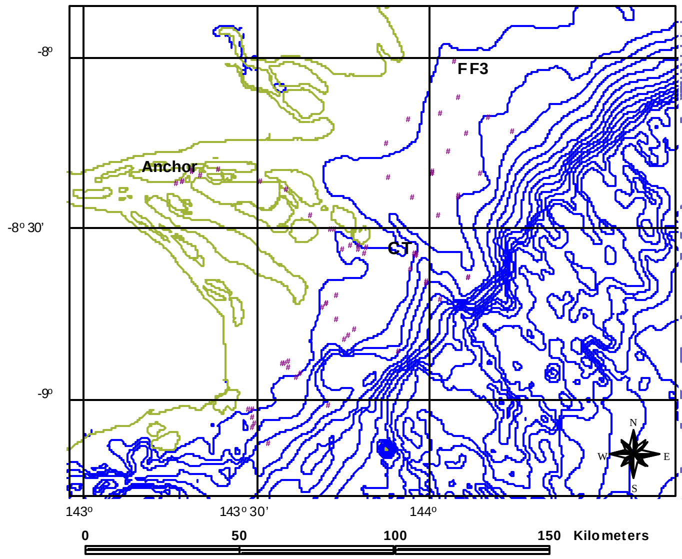

Figure 1. Study area and stations occupied during the January 2003 cruise.

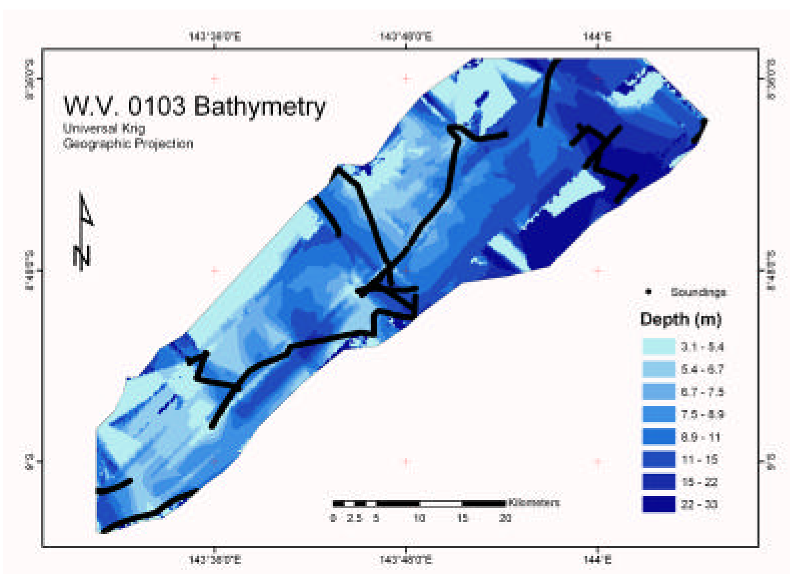

Figure 2. Bathymetric grid of fathometer soundings. Channels can be clearly seen as darker color values that trend northwest/southeast and cut across the delta front.

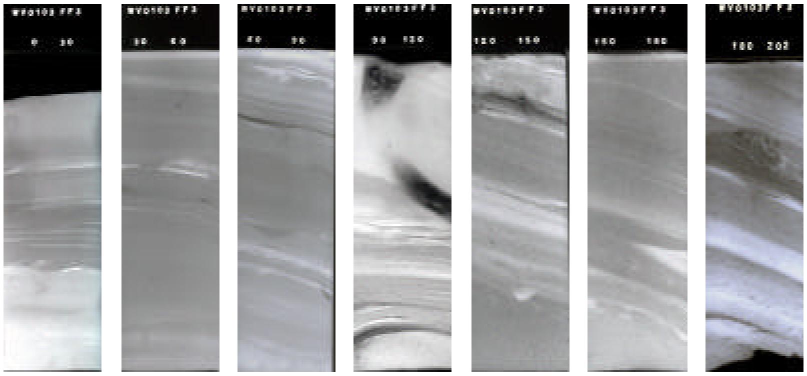

Figure 3. Photographs of the internal structure of core FF3. Darker areas indicated finer-grained sediment, light areas are sandier. Note the absence of biological structures such as burrows. Small dark 'cracks' near the bottom of the core are the result of degassing during retrieval of the core.

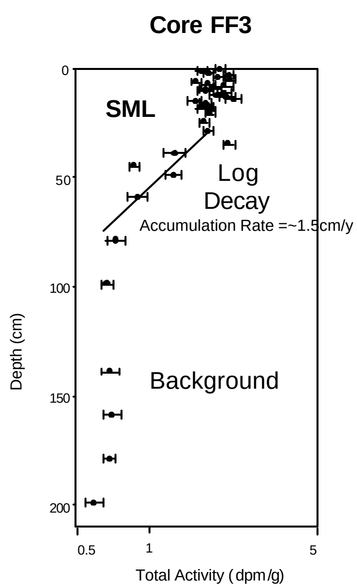

Figure 4. ^{210}Pb profile of core FF3.

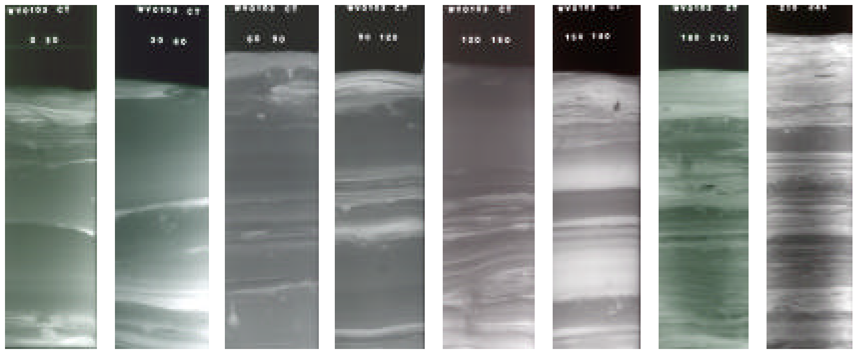

Figure 5. Photographs of the internal structure of core CT. Darker areas indicated finer-grained sediment, light areas are sandier. Note the absence of biological structures such as burrows. Small dark 'cracks' near the bottom of the core are the result of degassing during retrieval of the core.

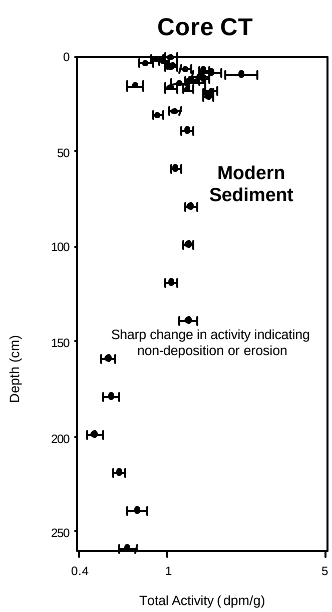

Figure 6. ^{210}Pb profile of core CT.

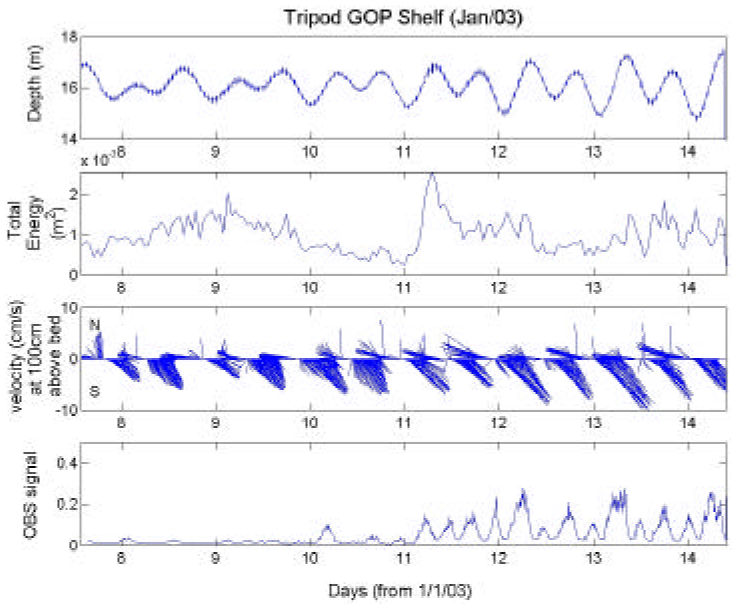

Figure 7. Data collected by the benthic tripod deployed at station CT in 16.7 m water.

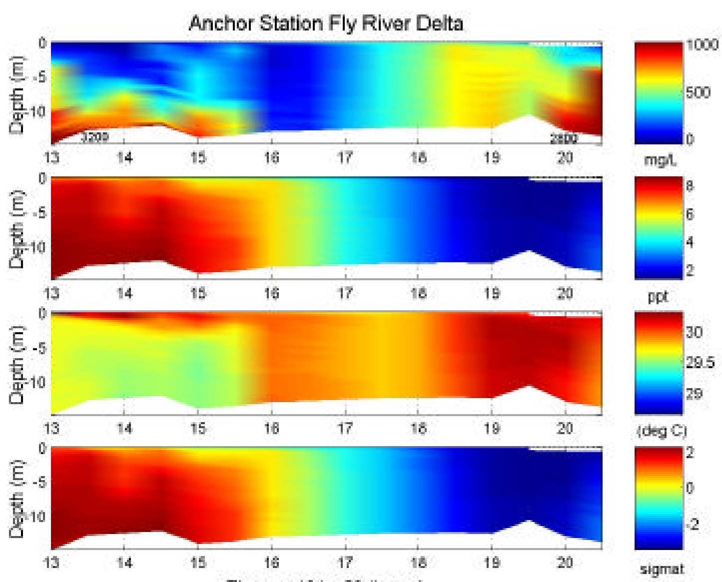

Figure 8. Suspended sediment concentration (mg/L), salinity (ppt), temperature (deg C) and Sigma T at the anchor station.

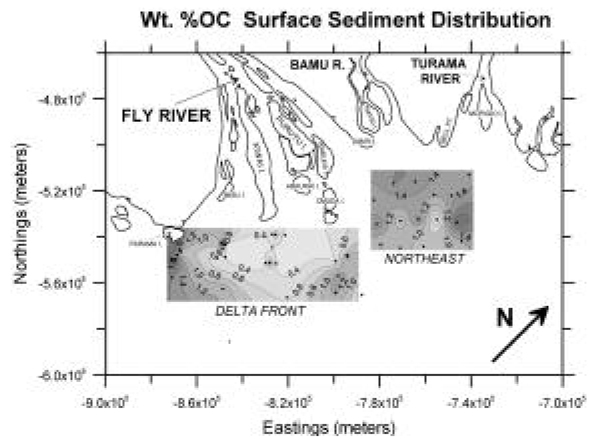

Figure 9. Weight percent of organic carbon associated with the surface sediments.

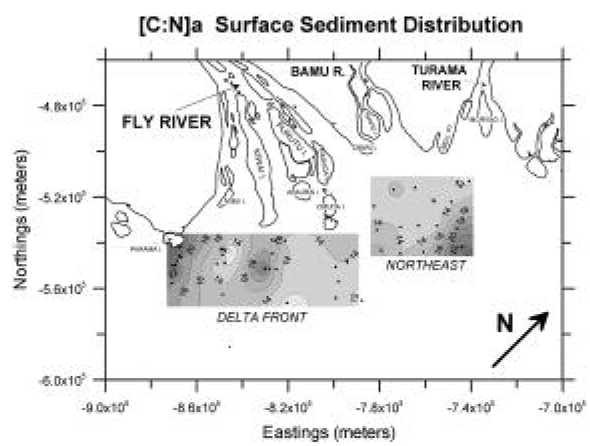

Figure 10. [C:N]a in the surface sediment.

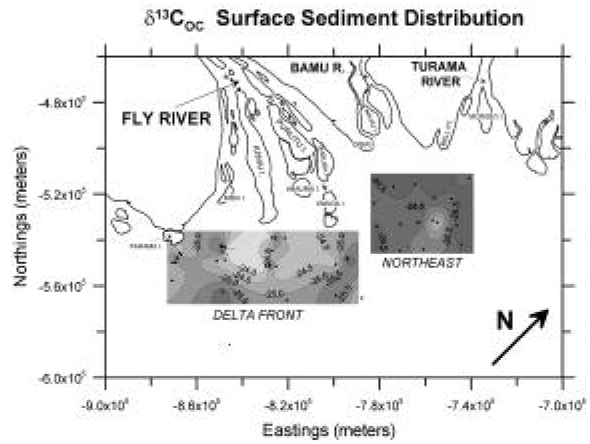

Figure 11. del$^{13}C_{OC}$ in surface sediments.

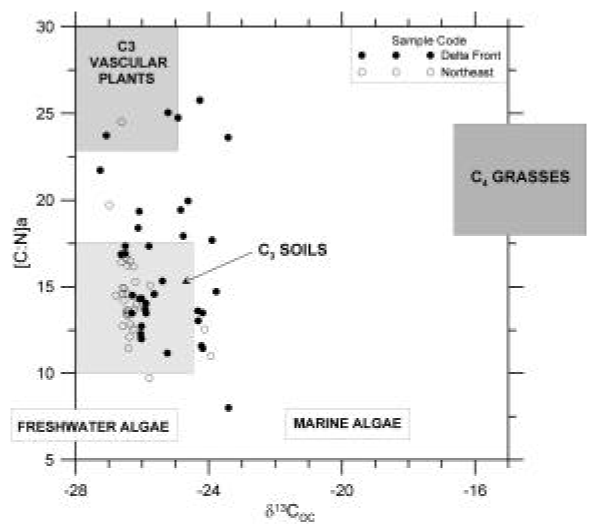

Figure 12. Typical del$^{13}C_{OC}$ and [C:N]a values for different sources to the marine environment.

Station	Longitude	Latitude	Station	Longitude	Latitude	Station	Longitude	Latitude
AA5	143.87930	-8.34708	A1	143.71312	-8.39377	C1-10	144.11286	-8.64292
AA7	143.95400	-8.40483	A2	143.71202	-8.33100	C2-8	143.95766	-8.57433
AA9	144.02354	-8.45053	A3	143.71118	-8.27752	Tripod	143.96361	-8.57557
BB9	144.08725	-8.40510	A4	143.66437	-8.27783	C3-12	143.94455	-8.62353
BB7	144.01211	-8.32974	A5	143.66482	-8.32747	C2-A11	143.99376	-8.65592
BB5	143.88757	-8.24579	A12	143.65863	-8.45917	anchor1	144.03831	-8.67595
BB3	143.84528	-8.20341	A11	143.58486	-8.38142	E1	143.60530	-8.94813
CC3	143.89442	-8.13974	A10	143.51292	-8.35957	E2	143.61492	-8.93398
CC5	143.94173	-8.17957	A9	143.38860	-8.32400	E3	143.62449	-8.92329
CC7	144.05790	-8.27530	A8	143.27329	-8.36042	E6	143.57981	-8.89281
CC9	144.14716	-8.33545	A8.5	143.28637	-8.36194	E7	143.59157	-8.88679
DD9	144.18040	-8.27833	A6	143.06540	-8.40450	E5	143.57381	-8.89634
DD7	144.10971	-8.22340	A7	142.89791	-8.37370	E4	143.59534	-8.90781
DD5	144.03082	-8.16339	apex	142.72612	-8.31258	G1	143.48472	-9.07766
DD3	143.96027	-8.10326	Anchor2	143.31404	-8.32382	G2	143.49303	-9.06848
EE9	144.23847	-8.21453	B3	143.79660	-8.59492	G4	143.47679	-9.03119
EE7	144.17257	-8.17522	B4	143.81313	-8.57385	G5	143.48697	-9.03150
EE5	144.08216	-8.11661	B5	143.82083	-8.55520	G3	143.48510	-9.05211
EE3	144.00739	-8.05988	B6	143.78700	-8.54473	G15	143.53478	-9.12881
FF3	144.07288	-8.00982	B7	143.77357	-8.54842	E15	143.70745	-9.01747
			B8	143.74963	-8.55737	D1	143.75414	-8.82558
			B9	143.74958	-8.52527	D2	143.76579	-8.81333
			B10	143.75203	-8.49652	D5	143.72975	-8.69383
			B11	143.72773	-8.50193	D7	143.69168	-8.72808
			B12	143.71070	-8.50200	D3	143.78535	-8.79666
			Z1	143.33527	-8.34567	D6	143.70188	-8.72002
			Z2	143.31168	-8.33503	D4	143.72942	-8.76392
						D15	143.91090	-8.86026
						C30	144.03294	-8.70910
						CT	143.96330	-8.57642

Table 1. Coordinates of stations occupied.